

## Simulations of beryllium erosion-re-deposition and tritium retention in the ITER main chamber using LIM-DIVIMP

S.Carpentier<sup>1</sup>, S. Lisgo<sup>1</sup>, J.D. Elder<sup>2</sup>, A.S. Kukushkin<sup>1</sup>, R.A. Pitts<sup>1</sup>, P.C. Stangeby<sup>2</sup>

<sup>1</sup> ITER Organization, Route de Vinon sur Verdon, 13115 Saint Paul Lez Durance, France

<sup>2</sup> University of Toronto Institute Aerospace Studies, Ontario M3H 5T6, Canada

**1. Introduction** Even if detailed results vary between machines, most current devices operating in single-null diverted configurations provide a similar picture of long-term material migration in which the inner divertor is a region of net deposition and the main chamber is generally a zone of net erosion. However, the expected migration picture in ITER could be one of the many aspects that differentiate this future machine from present day devices. Unlike any current operating tokamak, ITER will operate long pulse and high performance discharges in a Be/W environment, with a high upper triangularity (leading to divertor-like plasma-wall interaction at the top of the main chamber) and with a close fitting first wall (FW), Fig. 1a. The latter will consist of 440 massive blanket modules (BM, Fig. 1b), each protected by a separable and actively cooled Be panel (low Z material), for a total of  $\sim 700 \text{ m}^2$  of Be facing the plasma.

Each panel will consist of a double winged structure [1,2], toroidally (and sometimes poloidally) shaped (Fig. 1b-c) to protect leading edges from the impact of plasma flux. This shaping leads both to shadowed regions where material can potentially re-deposit without subsequent re-erosion, and to locally increased erosion rates due to the steeper attack angles of plasma fluxes. This dual FW shaping effect, coupled with the low sputtering threshold of Be and its relatively high tritium (T) co-deposition efficiency, is a matter of concern from the point of view both of FW erosion lifetime and main chamber fuel retention given the high fluence that will characterize burning plasma operation on ITER. This issue is the subject of dedicated modeling activity within the ITER Organization.

**2. First local modelling using LIM** The most recent ITER  $Q_{DT}=10$  burning plasma reference magnetic equilibrium (15 MA, inductive, H-mode steady-state phase) is illustrated in Fig. 1a. In this reference equilibrium, relatively close to double-null configuration, the distance between the first and second separatrices is  $\Delta R_{sep} \sim 10 \text{ cm}$  at the outer midplane (omp). The most intense plasma-main chamber wall interactions occur at the top of the main chamber, where the secondary scrape-off layer (SOL) intersects the upper modules (mainly BM#8-9). The poloidal curvature of the magnetic flux surfaces on the low field side (LFS) also creates a thin, “banana-shaped” SOL region delimited by the intersection of the first limited flux surface (FLFS) with BM#11 and 18. The second separatrix and the FLFS are radially very close together, separated by  $< 2 \text{ cm}$ .

In a first attempt at modelling main chamber Be erosion and associated T-retention, an upgraded version of the 2D Monte-Carlo impurity transport code LIM, incorporating the toroidal shape of the FW panel, has been used to simulate the local erosion-re-deposition process in the toroidal-radial plane, on a single BM#11. This exercise, reported in [3], has been performed assuming a limiter-like contact on the outboard wall, thus ignoring the contact at the top of the main chamber, and using appropriate absorbers in the simulation domain to approximate particle losses that would occur in the real 3D system. Accounting for uncertainties in Be sputtering yields and imposed plasma conditions, these LIM calculations found net peak erosion in the range  $4 \times 10^{-4} \rightarrow 0.06 \text{ mm/h}$  of Be, showing that first wall PFC lifetime due to steady-state operation alone could be an issue for ITER. This first study has also shown that net erosion due to both charge-exchange (CX) neutral sputtering (assuming uniform CX fluxes =  $4.2 \times 10^{21} \text{ m}^{-2} \cdot \text{s}^{-1}$  with average energy  $\langle E_n \rangle = 25 \text{ eV}$  from EIRENE

simulations) and to a time-averaged (controlled) ELM contribution (weighted according to its duration, equivalent to  $\sim 3.5\%$  of the 400s flat-top in ITER, assuming mitigated ELMs with power deposition time of  $\sim 0.5$  ms, and ELM frequency  $\sim 70$  Hz [1,6]) is locally negligible compared to the wear induced by ions from the steady-state (inter-ELM) plasma. These two contributions are thus ignored for the further medium-scale simulations presented in this paper. In addition, the first local LIM study demonstrated that local Be re-deposition does occur, confirming that a close fitting, shaped Be first wall can promote significant main chamber T-retention (up to  $\sim 3$  gT/h in some locations). This initial modelling attempt has been successfully benchmarked with the 3D ERO code for equivalent input parameters, providing confidence that the simulations are reasonable [4], even if both approaches obviously suffer from the inherent uncertainty in the input parameters (essentially erosion yields and local plasma parameters). The good agreement between 2D and 3D analysis was not unexpected since the large scale size involved, relative to ionization lengths and plasma poloidal cross-field gradient lengths, makes the problem quasi-2D. However, because the largest FW steady-state particle loads will in reality occur at the top of the machine, in the vicinity of BM#8-9, only simulation of the more complex divertor-like interactions with the upper BMs can provide a more realistic assessment of the likely magnitude of main chamber erosion-re-deposition.

**3. DIVIMP “medium-scale” modelling on multiple upper panels** A second and more advanced “medium-scale” model has now been developed using the 2D DIVIMP code (traditionally used for simulations in the poloidal-radial domain), allowing both the recessed areas of multiple toroidally-shaped upper panels and the divertor-like magnetic configuration in that region to be accounted for. Significant modifications to DIVIMP have been required to permit the definition of computational grids in a new  $[\rho, s]$  coordinate system, where  $\rho$  is the radial distance from the second separatrix at the origin (see below), and  $s$  is the parallel distance along the field line. To derive these grids, 3D field line tracing has been performed, beginning from 300 points at each of 20 radial origins chosen at different radial-poloidal locations across the central slot of one BM#9 unit. The intersections of the field lines launched from each of these points of origin with the 3D FW geometry provide the  $(\rho, s)$  matrix required to generate “distorted” linear grids for DIVIMP (an example of which is shown in Fig. 2b). Since the DIVIMP code is 2D, only a single and isolated medium-scale slice (or grid) can be represented at a time so that the ensemble of simulations used to map out the 3D pattern are not coupled, in contrast to transport in the real situation. This was the technique used in [3] to construct the erosion-deposition profiles across the full face of an isolated BM#11, whilst the ERO benchmark in [4] was able to treat the full 3D module in a single simulation. Radial absorbers, placed at the second separatrix radius for each grid, have also been added to simulate particle leakage toward the lower divertor and remote main chamber areas.

The plasma profiles (density and temperature) specified in these DIVIMP simulations correspond to the lowest (LDC) and highest (HDC) inter-ELM (static) ion flux conditions adapted for the reference equilibrium and baseline operating conditions in [3] from the definitions in the ITER “Heat and Nuclear Load Specifications” [5]. Outside the second separatrix, the SOL profiles are derived taking into account the full radial dependence of the connection lengths in the presence of the shaped wall, yielding a sharp drop of density in the recessed regions of the wall. In addition, since the width of the flux tubes increases at the top with respect to the  $omp$  (in the poloidal plane), the SOL decay lengths in the secondary divertor region have been increased to account for the magnetic flux expansion factor ( $F_{exp} = (B_\theta/B_\phi)_{omp}/(B_\theta/B_\phi)_{BM9} = 0.3/0.05 = 6$ ). The simulations assume an isothermal (sheath limited) far-SOL plasma with radially-flat temperature profiles (consistent with the convective, filamentary transport observed in the far SOL of modern tokamaks). Cross-field impurity

particle diffusion coefficients of  $D_{\perp} = 3 \text{ m}^2 \cdot \text{s}^{-1}$  are used for both LDC and HDC with no imposed background parallel SOL flow. The D→Be and Be→Be sputtering yields correspond to the Eckstein calculated and angle-averaged yield database found in [6], which are consistent with laboratory erosion yield measurements [7] and those found in the divertor region of JET during operation with Be targets [8].

**4. Results and discussion** Although the level of approximation is still significant with this new approach, this medium-scale modelling does capture the plasma footprint on the FW panels resulting from internal (to each panel) and nearest neighbour BM shadowing, in addition to tracking the multiple “private flux regions” between modules (see Fig. 2b). As a result, the simulations do allow the Be migration process between neighbouring panels to be studied, a feature absent in the isolated BM studies performed with LIM. The new medium-scale model has first been successfully cross-checked against the LIM BM#11 isolated model simulation for equivalent input parameters (Fig. 2a). Preliminary DIVIMP results for the new medium-scale approach are shown in Fig. 2c-d for the HDC on BM#9. The simulated net erosion and deposition patterns obtained for both LDC and HDC show net erosion close to the BM tip (where the incident angles are small, ~6°), with a maximum net peak Be erosion ranging between  $\sim 1.3 \times 10^{-3} \text{ mm/h}$  (LDC) and 0.015 mm/h (HDC), corresponding to a PFC lifetime of approximately [3600 – 42 000] shots (assuming an allowed-eroded thickness of 6 mm before end-of-life on any given Be tile of the FW panel). The respective ratios of peak net to gross erosion for HDC (LDC) are up to 0.4 (1.0), very different from the situation in the primary divertor (where net erosion is usually either close to zero or very negative), and the origin of biggest concern for FW PFC lifetime. Contrary to the situation simulated on outboard BM11 in [3], net deposition on the upper modules does not occur in shadowed areas, but mainly in regions wetted by the plasma, meaning that most of the co-deposition would occur at the top of the machine in regions where surface temperatures will be quite high. This is advantageous in the sense that less T is retained for higher co-deposition temperature [9], but the gain is to some extent offset by the higher baking temperatures required to release fuel deposited at elevated surface temperature [10]. The non-local re-deposition fraction due to particles lost inboard of the second separatrix by the radial absorbers, or re-deposited on neighbouring rows BM#8-11 is only ~15% for HDC. This result is in agreement with  $^{13}\text{C}$  labelled methane injection experiments performed on the DIII-D tokamak [11], in which strongly localised re-deposition was observed in the secondary divertor region of ITER-like plasma configurations under relevant plasma conditions. For LDC, >70% of the eroded particles are lost to the SOL plasma. The T-retention rates associated with the estimated local Be re-deposition on top panels will be estimated later, once the full surface temperature map corresponding to the assumed plasma loading profile has been properly computed. The modelling work presented in this paper is still in progress. A full sensitivity study is currently on-going to assess the influence of different inputs ( $D_{\perp}$ , plasma flows, Be sticking factor, magnetic configuration with different  $\Delta R_{\text{sep}}$  or upper X-point position, uncertainties in sputtering yields and co-deposition ratios, etc.).

**References** [1] R. Mitteau et al., J. Nucl. Mat. (2011), in press [2] P.C. Stangeby et al., J. Nucl. Mat., 390–391 (2009) 963–966 [3] S. Carpentier et al., J. Nucl. Mat. (2011), in press [4] D. Borodin et al., 2011 PFMC Conf. Proc. [5] R. Pitts et al., J. Nucl. Mat. (2011), in press [6] W. Eckstein, Report IPP 9/132 (2002) Garching [7] J. Roth et al., Fus. Eng. Design, 37 (1997) 465–480 [8] M.F. Stamp et al., J. Nucl. Mat. (2011), in press [9] G. De Temmerman et al., Nucl. Fusion 49 (2009) 042002 [10] K. Sugiyama et al., J. Nucl. Mat. (2011), in press [11] J.D. Elder et al., J. Nucl. Mat. (2011), in press

**Disclaimer** The views and opinions expressed herein do not necessarily reflect those of the ITER Organization.

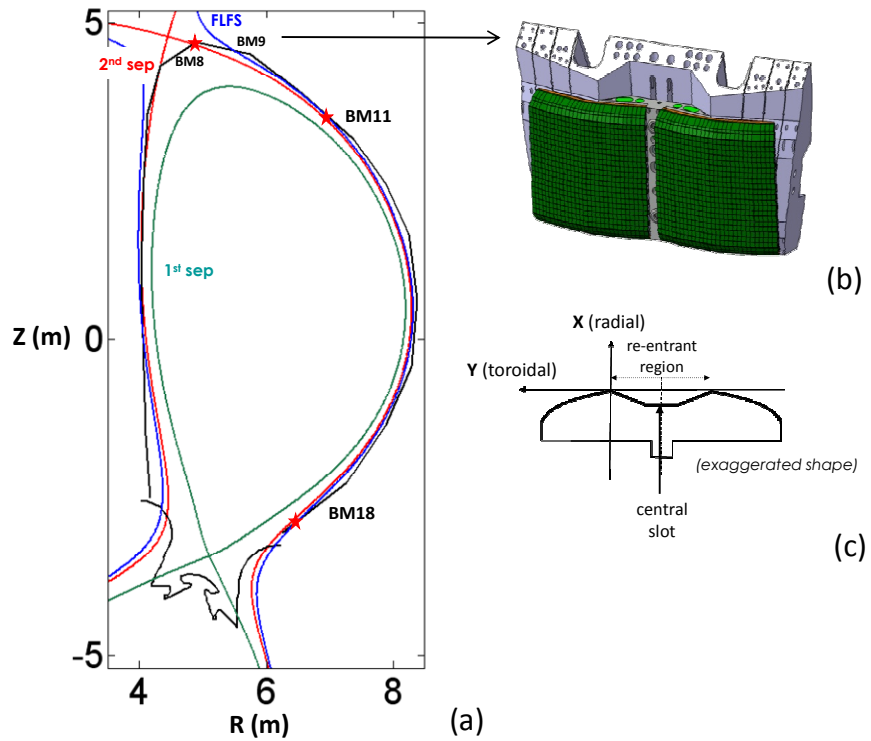


**Fig. 1** (a) ITER baseline magnetic equilibrium for 15 MA  $Q_{DT} = 10$  scenario with first separatrix (in green), second separatrix (in red) and FLFS (in blue) – The location of the reference BM numbers used in this paper are shown in this picture (b) 3D CAD view the ITER first wall BM#9 (c) Exaggerated view of the BM toroidal shaping

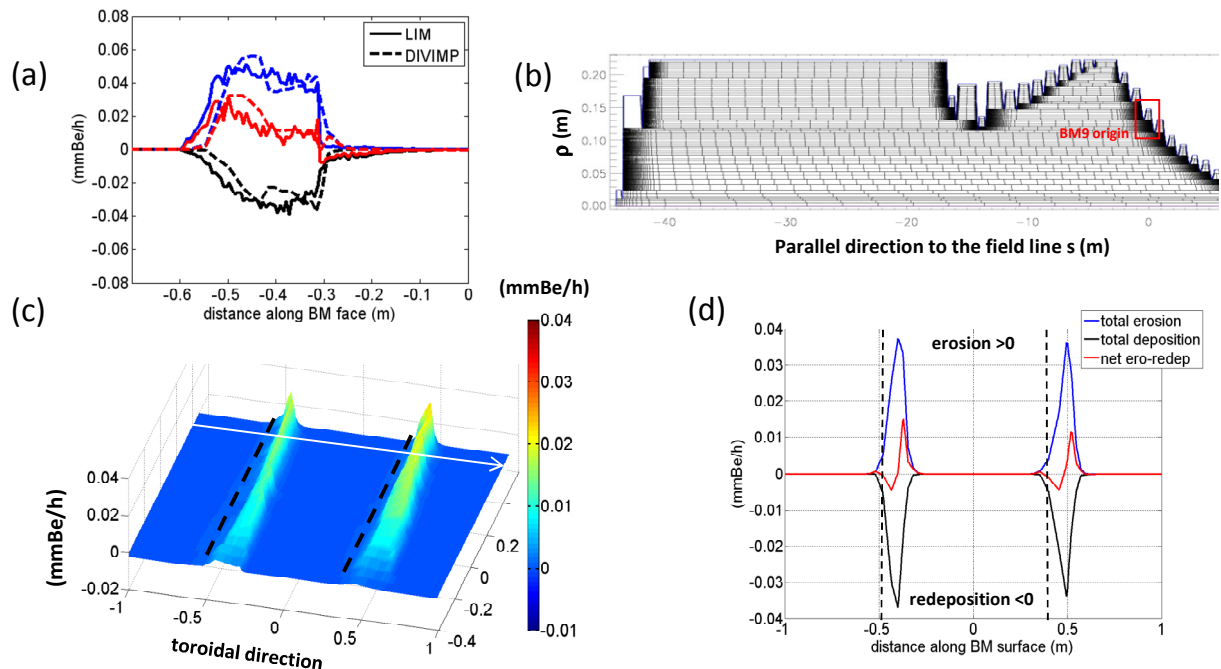


**Fig. 2** (a) DIVIMP erosion-redeposition profiles on BM11 cross-checked against previous LIM results for HDC (b) One 2D linear “distorted” grid generated in DIVIMP in the new ( $\rho, S$ ) referential (c) 2D net erosion-redeposition pattern assessed on BM#9 for HDC (d) Detailed profiles of total erosion, net erosion and total deposition due to inter-ELMs ion fluxes on BM#9, along the toroidal slice shown in Fig. 2c.